Quantifying the acceleration of multidecadal global sea surface warming driven by Earth's energy imbalance

ENVIRONMENTAL RESEARCH
LETTERS

PURPOSE-LED PUBLISHING™

LETTER • OPEN ACCESS

Quantifying the acceleration of multidecadal global sea surface warming driven by Earth's energy imbalance

To cite this article: Christopher J Merchant *et al* 2025 *Environ. Res. Lett.* **20** 024037

ENVIRONMENTAL RESEARCH
LETTERS

OPEN ACCESS

RECEIVED
2 October 2024

REVISED
30 December 2024

ACCEPTED FOR PUBLICATION
15 January 2025

PUBLISHED
28 January 2025

LETTER

Quantifying the acceleration of multidecadal global sea surface warming driven by Earth's energy imbalance

Christopher J Merchant*, Richard P Allan and Owen Embury

National Centre for Earth Observation, University of Reading, Reading, United Kingdom
* Author to whom any correspondence should be addressed.

E-mail: c.j.merchant@reading.ac.uk

Keywords: acceleration, global, energy, ocean, temperature, warming

Abstract

Global mean sea surface temperature (GMSST) is a fundamental diagnostic of ongoing climate change, yet there is incomplete understanding of multi-decadal changes in warming rate and year-to-year variability. Exploiting satellite observations since 1985 and a statistical model incorporating drivers of variability and change, we identify an increasing rate of rise in GMSST. This accelerating ocean surface warming is physically linked to an upward trend in Earth's energy imbalance (EEI). We quantify that GMSST has increased by 0.54 ± 0.07 K for each GJ m^{-2} of accumulated energy, equivalent to 0.17 ± 0.02 K decade^{-1} (W m^{-2})$^{-1}$. Using the statistical model to isolate the trend from interannual variability, the underlying rate of change of GMSST rises in proportion with Earth's energy accumulation from 0.06 K decade^{-1} during 1985–89 to 0.27 K decade^{-1} for 2019–23. While variability associated with the El Niño Southern Oscillation triggered the exceptionally high GMSSTs of 2023 and early 2024, 44% (90% confidence interval: 35%–52%) of the +0.22 K difference in GMSST between the peak of the 2023/24 event and that of the 2015/16 event is unexplained unless the acceleration of the GMSST trend is accounted for. Applying indicative future scenarios of EEI based on recent trends, GMSST increases are likely to be faster than would be expected from linear extrapolation of the past four decades. Our results provide observational evidence that the GMSST increase inferred over the past 40 years will likely be exceeded within the next 20 years. Policy makers and wider society should be aware that the rate of global warming over recent decades is a poor guide to the faster change that is likely over the decades to come, underscoring the urgency of deep reductions in fossil-fuel burning.

1. Introduction

For 450 d during April 2023–July 2024, near-global mean sea surface temperatures (GMSSTs) exceeded previous observed seasonal maxima by up to 0.31 K and by 0.18 K on average. As was previously observed during 1997/98 and 2015/16, a change from the La Niña conditions prevalent during 2021/22 to the strong El Niño phase that emerged in early 2023 was associated with marked new highs in GMSST in 2023/24. However, the record high GMSSTs in 2023/24 exceeded what would be inferred by analogy with those earlier El Niño episodes (see table 1; for the data used, see section 2). As quantified by the El Niño Southern Oscillation (ENSO) 3.4 index, the 2023/24 El Niño was weaker than in 1997/98, yet the recent event was accompanied by notably greater duration and amplitude of record-breaking GMSSTs. The objective of this paper is to account for this by quantifying the multidecadal acceleration of ocean mixed-layer warming that combined with interannual variability to cause the exceptional SSTs in 2023 and 2024.

The SST events of 2023/24 have been discussed in several contexts. The GMSSTs observed corresponded to ocean heat content (OHC) in the Tropical Atlantic Ocean, Mediterranean Sea, and Southern Ocean greater than previously observed in records since the 1950s [1]. The extreme GMSST has been characterised as a 4-sigma event by Kuhlbrodt *et al* [2], who also noted that the north Atlantic warmth was more consistent with a 3 °C global-warming scenario than with the prevailing climate. The increase

Table 1. Comparison[a] of strong El Niño events and their GMSST impact.

Event	Δ ENSO 3.4	Duration of GMSST record (d)	Maximum GMSST record (K)	Mean GMSST record (K)	Degree-days of GMSST record (K d)
2023/24	2.7	450	0.31	0.18	82.2
2015/16	2.9	428[b]	0.31	0.13	55.7
1997/98	3.2	374[c]	0.21	0.12	44.2

[a] Statistics characterise in each case the period during which GMSST exceeded all previous GMSST values in the record (starting in 1980) for the given day of the year. The periods are the consecutive days of record GMSST, except for short interruptions noted below. 'ΔENSO 3.4' is the peak ENSO 3.4 index minus the average of the index during a full calendar year of preceding La Niña conditions (2022, 2013 and 1996; 2014 featured an aborted El Niño event, so 2013 is used as the comparator).

[b] Combines two sub-periods interrupted by 6 non-record days in late June of 2015.

[c] Combines two sub-periods interrupted by 3 non-record days in May of 1998.

in OHC in the ocean mixed layer must be accounted for by a combination of upwards heat flux from the deeper ocean and downward net heat flux at the ocean's surface. The net surface influx of energy is sustained by Earth's energy imbalance (EEI), which is the imbalance between the energy absorbed and emitted by the Earth [3–5]. While ongoing increases in greenhouse gas concentrations tend to increase EEI [6], reduced anthropogenic atmospheric aerosols have also been implicated in the increasing EEI since ∼2010 [7], although the precise role of aerosols in the observed reduction in planetary albedo remains difficult to demonstrate [4, 8]. The positive radiative forcing from stratospheric water vapour injected by the Hunga Tonga eruption was considered a potential contributor to increased GMSST [9], but accounting for the negative forcing from stratospheric aerosol from the eruption [10] suggests a minor temperature impact.

After the description of our data and methods in section 2, the narrative of this paper is as follows. There is reason to hypothesize an acceleration in ocean warming given observations of EEI (section 3). This acceleration of GMSST warming is, for the first time, demonstrated statistically and quantified in section 4. The implications are (i) that this acceleration was significant in the exceptional SSTs of 2023 and 2024 (section 5.1), and (ii) that expectations for future climate in the coming decades are significantly changed when one accounts for acceleration of SST rise, compared to assuming steady warming in line with recent decades (section 5.2).

2. Data and methods

Monthly global-mean all-sky net-downward radiative fluxes, quantifying EEI, were obtained from the Clouds and the Earth's Radiant Energy System (CERES) Energy Balanced and Filled Top-of-Atmosphere edition 4.2 version 3 dataset ('CERES EEI'), covering March 2000–April 2024 [11, 12]. CERES measures outgoing radiances that are converted to fluxes and combined with Solar Radiation and Climate Experiment incoming solar radiation observations to estimate the top-of-atmosphere radiation balance. Since the absolute accuracies of the satellite instruments are insufficient to quantify imbalances ∼1 W m^{-2}, the heat content of the upper 2000 m of the ocean and other assumptions are used to estimate the absolute EEI [13]. Although this CERES EEI is anchored to OHC, the temporal variations and regional coverage provide independent information. The systematic 0.2 W m^{-2} uncertainty in EEI primarily relates to uncertainty in OHC, while observational stability uncertainty is $<$0.1 W m^{-2} $decade^{-1}$.

From January 1985 to February 2000, we use an adjusted monthly global mean of the DEEP-C version 5 reconstruction of EEI [14, 15]. DEEP-C combines an earlier CERES release with reanalyses and Earth Radiation Budget Satellite measurements, with temporal gaps in 1993 and 1999 constrained with modelling. Seasonal-cycle adjustments to the DEEP-C data are applied based on the overlapping complete years between DEEP-C and CERES Ed4.2 (March 2000–February 2020). Before the CERES epoch, the uncertainty is 0.5 W m^{-2}.

'Global' mean SST herein means the area-weighted average SST between 60°S and 60°N, excluding inland seas, following a common convention [16]. This GMSST definition minimizes ambiguities in the meaning of SST in areas of sea-ice cover. Monthly mean GMSST is calculated from the European Space Agency Climate Change Initiative SST analysis product. This is a daily, gap-filled satellite-derived climate data record [17, 18], extended routinely as an interim climate data record, with a combined time span of January 1980–July 2024. Here, as for all variables, data prior to the start of the DEEP-C record in January 1985 are not used.

EEI and SST have annual cycles [19] that are not the focus here, and timeseries are deseasonalised prior to analysis.

Multivariate regression by ordinary least squares is used to fit timeseries $y(t)$. The fitted values, $f(t)$, are linear combinations of predictors, $p_i(t)$: $f(t) =$

$\sum_1^n a_i p_i(t)$. The process model [20] of the timeseries is $Y(t) = F(t) + E_o(t) + E_v(t)$, where additional processes represent observation errors (E_o) and components of GMSST variability (E_v) not fitted by the processes included in F via predictors.

Estimated uncertainties in the GMSST parameters reflect three assumptions: (i) GMSST observations have negligible noise (because independent random errors in the resolved SSTs average to negligible levels in the global monthly average); (ii) GMSST values are subject to observational stability errors, representable by an error covariance matrix; (iii) unfitted natural variability is present, the amplitude and autocorrelation of which are accounted for in the parameter uncertainty. The total parameter uncertainty is estimated by combining the observational stability uncertainty and uncertainty from unfitted variability.

The observational stability uncertainty is estimated by propagating an error covariance matrix for E_o through the regression. This error covariance matrix corresponds to: (i) an uncertainty of 0.02 K (0.05 K prior to January 1993) in the global mean SST; and (ii) an assumed linear decrease of error correlation to zero at 120 months' time separation. This corresponds to GMSST biases having a persistence of order one decade, comparable to the length of many satellite missions that contribute to the record.

The fitting uncertainty is estimated using a bootstrap algorithm [20] that accounts for the impact on uncertainty of autocorrelation in residuals.

Some predictors $p_i(t)$ are functional forms, such as linear, piecewise linear and quadratic curves. Piecewise linear predictors in two parts (a 'break model' [20],) involve objectively determining the break time (the time at which the linear slope changes) that minimises the summed squares of the fit residuals across all possible times.

Non-functional predictors are derived from timeseries of factors that explain some of the GMSST variability [21]. Positive ENSO phases are associated with higher GMSST and negative events with lower GMSST. Positive and negative phases are used as separate predictors to avoid imposing symmetry of GMSST impacts. The SST anomaly for 170–120°W and 5°S to 5°N, i.e. the ENSO 3.4 index, is used as the predictor, derived from the spatially resolved SSTs and lagged by 3 months to account for a delayed influence on global climate [21]. Lags from 0 to 5 months were tested using the linear model, and 3 months' lag minimised the summed squares of the residuals. Using a 'normalised' ENSO index [22] that avoids aliasing the global warming signal was tested but did not improve the model fits.

Variable solar irradiance is included using a merged daily total solar irradiance timeseries [23]; at time of access, data were available to April 2024 and were extended with the value of the last month. Stratospheric volcanic aerosol effects on GMSST are obtained by exponential smoothing of daily area-weighted-mean aerosol optical depths in GLOSSAC v2.0 [24] followed by monthly averaging. The time-constant for the smoother is 142 d, the optimum of several tested values between 3 and 7 months. The sensitivity of the results to this parameter is very small. This dataset ends in December 2018, and thereafter a constant background value is applied. The Hunga Tonga eruption of 2022 is neglected, since the net GMSST effect is likely to be small [10].

In calculations involving the areal heat capacity of mixed-layer seawater, we use the approximations of constant specific heat capacity (3990 J K^{-1} kg^{-1}) and density (1032 kg m^{-3}).

3. Accumulation of energy in the Earth system

A sustained positive EEI implies accumulation of energy as heat in the Earth system. This accumulating energy is partitioned primarily into the oceans [25] where increases in OHC contribute to sea-level rise through steric expansion of seawater [26]. The global mean EEI has been estimated in budget closure studies to be: 0.48 ± 0.1 W m^{-2} for 1971–2020 and 0.76 ± 0.2 W m^{-2} for 2006–2020 [25]; 0.50 ± 0.43 W m^{-2} for 2001–2010 [13]; 0.5 ± 0.2 W m^{-2} for 2000–2009 and 1.0 ± 0.2 W m^{-2} for 2010–2019 [27], suggesting an increase in EEI over recent decades.

Figure 1 shows the monthly deseasonalised global area-weighted mean EEI, using CERES since March 2000 and DEEP-C prior (see section 2). The time-average and standard deviation of EEI are 0.80 ± 0.88 W m^{-2}. The reflective stratospheric aerosol layer that spread globally after the Mt Pinatubo eruption in 1991 [28] caused the most negative EEI months in the timeseries around 1992 [15, 29]. ENSO-related perturbations in EEI are also visible in 1998/9 and 2010/11.

The data show an upward trend, as noted in [27], of 0.45 ± 0.09 W m^{-2} $decade^{-1}$ during 2000–2022. Inspection of the time series suggests a faster increase later in the record. To test this hypothesis, we fit a piecewise-linear break model, for both the combined data and the CERES-only EEI. Both fits identify a break in the slope in 2010. The fits are nearly indistinguishable, figure 1(a). The EEI trend changes from 0.29 ± 0.08 W m^{-2} $decade^{-1}$ prior to July 2010 to 0.58 ± 0.18 W m^{-2} $decade^{-1}$ thereafter. The hypothesis of an increased slope is weakly supported, as the difference in slope is 1.4 times the uncertainty of the difference.

Time-integrating the EEI gives an estimate of Earth's energy accumulation (EEA), figure 1(b). The EEA curve has a marked quadratic component, while the increase in EEI slope and the interannual variability add higher-order terms. Around 1 GJ of energy

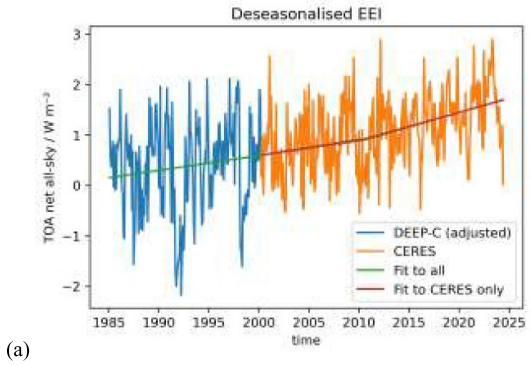

(a)

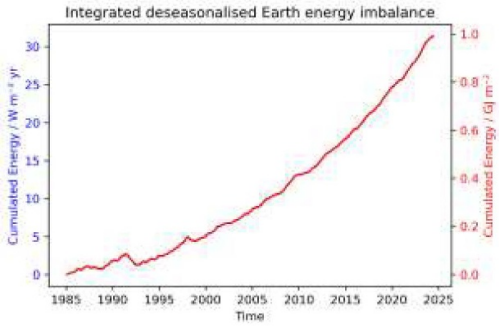

(b)

Figure 1. (a) Deseasonalised global-mean Earth energy imbalance. Piece-wise linear trend fits are based on combined DEEP-C and CERES data (green, with break point of July 2010) and CERES only (red, with break point at August 2010). (b) Earth energy accumulation (integrated EEI) from combined DEEP-C and CERES.

has been accumulated over ∼40 years for each square metre of Earth's surface.

4. Acceleration in global mean sea surface warming

The EEA warms the oceans, land, ice and atmosphere, and melts ice. We focus on the long-run implications of the EEA for SST.

SST is strongly coupled to the temperature of the mixed layer of the ocean. In the mixed-layer depth (MLD) climatology of Johnson and Lyman [30], the mean annual-maximum MLD between 60°S and 60°N is 91 m. This is an intuitive scale for the depth of ocean that determines an effective heat capacity on interannual timescales, and 100 m is often used in OHC analysis. The partitioning of energy between the mixed layer and deeper oceans is dynamic [31–33]. Large-scale modes of variability including ENSO and the Pacific Decadal Oscillation affect MLD, mixed-layer temperature, heat distribution and GMSST in complex ways. Thus, a direct relation of GMSST to EEA is not expected on interannual timescales.

The trend of GMSST over recent decades is commonly characterised as linear (e.g. [21, 34],). Samset *et al* [35] explicitly characterise the temperatures of 2023 as arising from internal variability 'in combination with steady anthropogenic global warming.' However, given figure 1(b), we hypothesize acceleration in the rate of GMSST increase, as has been noted for surface air temperature [36]. We next consider whether this acceleration can be detected in GMSST observations over the past four decades in the face of interannual variability.

The monthly GMSST timeseries since 1985 is shown in figure 2(a) (blue curve). The GMSST of the final year of the series is 0.9 K warmer than the first year. In line with the common characterisation, the warming appears consistent with a linear trend and interannual variability dominated by ENSO. To explore whether GMSST warming is accelerating, we fit three statistical models to the timeseries to assess whether models that include 'warming acceleration' are more convincing than a linear model.

The statistical models use identical predictors of monthly to multiannual variability (ENSO, stratospheric aerosol and solar irradiance) but differently represent the trend. The trend models are: linear, quadratic and proportional-to-EEA. For predictor details see section 2 and table 2. To compare statistical efficiency across the models, the sum of squares of residuals and number of parameters are shown in table 3. Lower residuals and fewer parameters indicate a more convincing model.

The linear model characterises the GMSST trend as a steady warming of 0.131 ± 0.015 K decade^{-1}. The quadratic model yields lower residuals, although a reduction is to be expected given the extra parameter. The quadratic coefficient is 0.026 ± 0.010 K decade^{-2}. The presence of acceleration in the time series is unambiguous, because the coefficient differs from zero by 2.6 times its uncertainty. Thus, GMSST acceleration is detectable, provided that interannual variability is modelled with informative predictors.

The fit using EEA to parameterise the trend is shown in figure 2(a) with its contributing components in figure 2(b). The warming trend captured by the EEA-proportional component amounts to 0.53 K over the 39.6 year period, matching the linear-model trend. However, the rate of increase rises from 0.06 K decade^{-1} over the first five years to 0.27 K decade^{-1} over the last five years. According to this model, the recent rate of underlying warming is therefore twice the 40 year mean trend.

The EEA coefficient is 0.17 ± 0.02 K decade^{-1}/(W m^{-2}), i.e. an EEI of 1 W m^{-2} that accumulates for 10 years increases GMSST (in the absence of sub-decadal variability) by 0.17 K. The EEI is a global imbalance, whereas only 63% of the Earth's surface between 60°S and 60°N is ocean, and only 89% of energy accumulated is stored in the ocean [25]. Accounting for these factors, the EEA coefficient implies 0.24 ± 0.03 K decade^{-1} per watt per square metre of ocean. The implied effective heat capacity per unit area [37] corresponds to a 323 m depth of ocean water—i.e. this is the depth of water which 1 W m^{-2} can heat uniformly at 0.24 K decade^{-1}.

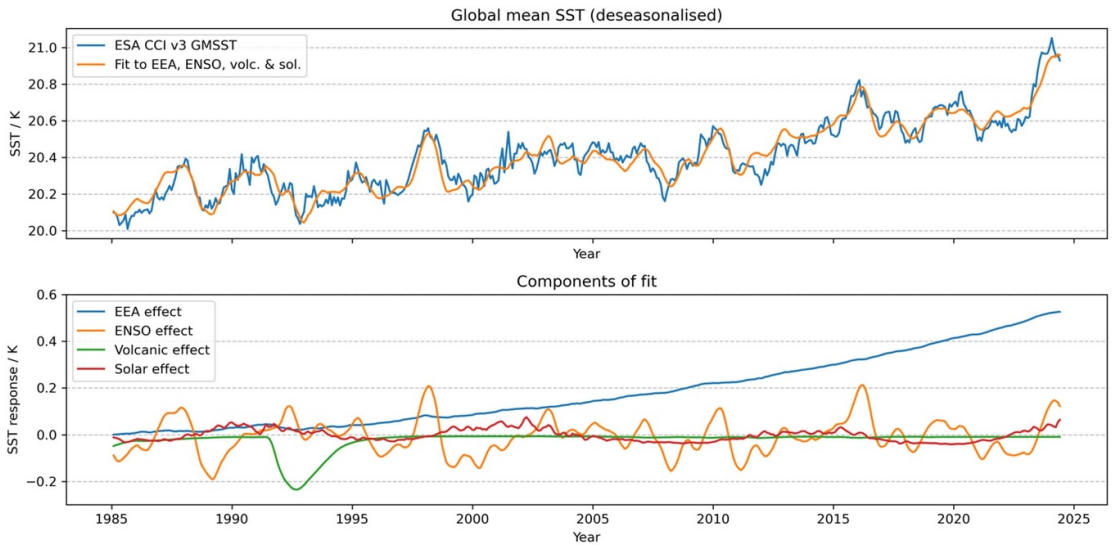

Figure 2. (a) Deseasonalised monthly mean sea surface temperature between 60°N and 60°S (GMSST). Blue line: observed timeseries from the European Space Agency Climate Change Initiative (ESA CCI). Orange line: fit to observed timeseries using Earth Energy Accumulation (EEA), El-Niño Southern Oscillation (ENSO) index, volcanic stratospheric aerosol and top-of-atmosphere total solar irradiance as predictors. (b) The components of the fit, i.e. the scaled predictors that (with an offset parameter not shown) sum to give the fitted curve in panel (a).

Table 2. Predictors used in fits of GMSST.

	Predictor	Comment
p_1	1	A time-invariant offset
$p_2(t)$	Linear term (if present): details below.	
$p_3(t)$	Acceleration (if present): details below.	
$p_4(t)$	ENSO 3.4 index > 0, lagged by 3 months	Value of index when positive, 0 otherwise
$p_5(t)$	ENSO 3.4 index < 0, lagged by 3 months	Value of index when negative, 0 otherwise
$p_6(t)$	Solar irradiance	Smoothed using a 3 month rolling window
$p_7(t)$	Volcanic aerosol, smoothed, lagged.	From mean stratospheric aerosol optical depth.
	Linear model	
$p_2(t)$	t	Whole-series linear trend
$p_3(t)$	N/A	No acceleration term
	Quadratic model	
$p_2(t)$	t	Linear trend
$p_3(t)$	t^2	Quadratic acceleration
	Earth Energy Accumulation model	
$p_2(t)$	N/A	No linear term
$p_3(t)$	EEA timeseries	SST trend driven by EEA

Table 3. Results of GMSST fits.

Model	Number of parameters	Sum of squares of residuals (K^2)
Linear-trend	7	2.18
Quadratic-trend	8	1.76
EEA-proportional trend	7	1.69

Correspondingly, 28% (90% CI: 23% to 35%) of the ocean heat uptake since 1985 is sufficient to heat the mean MLD of seawater at this rate. These relations of GMSST, mixed layer and EEA appertain to the EEI of the past ∼40 years, during which time the simple conceptual model of a fixed fraction of EEA driving the GMSST trend is shown to be useful. These parameters will describe future dynamics while broadly comparable EEI conditions prevail.

The fitted effects of solar irradiance and volcanic effects on SST are consistent with results in Lean and Rind [21], who fitted a linear trend to Earth surface temperature attributed to 'anthropogenic influence'. The results here, analogously to [36], show that a linear assumption is no longer convincing. A multi-decadal SST trend following the EEA provides a better account of GMSST in recent decades than an underlying linear process. The SST acceleration signal has emerged from the interannual variability.

5. Discussion

The GMSST underlying interannual variability is accelerating in proportion to the EEA on decadal timescales. Next, we discuss: (i) how this affects the interpretation of record-breaking GMSSTs in 2023/24; and (ii) the implications for future warming.

5.1. Recent record-breaking GMSST

Our results present 2023/24 GMSSTs as a consequence of a positive ENSO phase after sustained La Niña conditions, the dynamical response to solar-cycle forcing, and accelerating energy accumulation in the mixed layer that may reflect multiple drivers.

To assess the relative contributions, we compare the mean GMSST for November to January for the 2015/16 and 2023/24 El Niño events. The peak temperatures associated with El Niño occur towards the end of December. We address two questions: (i) 'Can the record SSTs of 2023/24 plausibly be explained with a linear trend in underlying GMSST?' and (ii) 'What is the role for vertical heat redistribution in the oceans, not captured by the GMSST model?'

Table 4 shows the components of temperature difference between the two El Niño events in the linear and EEA-proportional GMSST models, and compares their total to the observed difference between the events. The principal difference between the two models is in the trend component, which is the largest component in both cases. Because the latter ENSO event was weaker than the former, the ENSO effect reduces the temperature difference between the events, while this is partly offset by a positive solar-cycle effect. The EEA-based model predicts a 0.19 K temperature increase between the events, whereas 0.22 K was observed. The observational uncertainty in the difference is of order 0.01–0.02 K. The linear model, predicting merely 0.09 K difference, is unable to account for recent events.

Table 4. Temperature budget: GMSST differences between 2015/16 and 2023/24 peak ENSO (Nov–Jan mean).

Aspect of GMSST	Linear model (K)	EEA-based model (K)
Trend effect	+0.105	+0.199
ENSO effect	–0.060	–0.054
Solar effect	+0.038	+0.038
Total model fit	+0.087	+0.186
Observed	+0.215	+0.215
Total model fit—observed	–0.128	–0.029

The EEA-based model underestimates the temperature difference by 0.03 K, suggesting some residual unaccounted-for variability. Given the prolonged La Niña conditions prior to the 2023/24 El Niño, it is possible that a greater-than-usual amount of energy was subducted below the mixed layer during 2021 and 2022. If this energy returned to the upper ocean during the El Niño, this would cause a larger GMSST impact for a given ENSO 3.4 index at the ENSO peak. Allan and Merchant [4] expand on the plausibility of this using a spatially resolved analysis.

Overall, steady accumulation of heat in the mixed layer (a linear trend) fails to explain ∼0.1 K of the peak-ENSO temperature difference. The acceleration of mixed layer energy accumulation since 2015/16 is needed to account for the exceptional GMSSTs of 2023/24.

5.2. Future SST warming

This leaves unanswered the important question of what has caused the EEI trend. While the investigation of this crucial question is beyond the scope of this paper, the following brief comments contextualise the results in this section, where observation-driven scenarios of future warming are presented.

The EEI is the difference between the radiative forcing (positive) and the climate feedback response (negative). Radiative forcing from carbon dioxide and methane, the dominant greenhouse gases, has risen since 1985, with greater methane increases later in the record [38]. The shallow EEI trend prior to ∼2010 is attributed to the combination of this radiative forcing increase and the climate feedbacks in response. While greenhouse gas forcing has continued to increase since ∼2010, many authors have further noted that since then the negative radiative forcing from anthropogenic aerosols has decreased—an additional relative positive radiative forcing. The clean-up of terrestrial industrial sources and regulations to decrease the sulfur in shipping fuel have been discussed in connection to their radiative forcing effect [7, 39–43]. It is plausible that the additional EEI trend is driven by a change in aerosol radiative forcing, although analysis of the spatial characteristics of EEI changes also allow for a significant role for cloud-mediated feedback mechanisms over cloudy areas of ocean [4–6].

Here, we use these considerations to create indicative scenarios evolution of EEI/EEA and associated expectations for GMSST over the next two decades. This is done using the Earth energy accumulation model with predictors p_1 (the offset term), p_3, p_5 and p_6 (table 2). Our purpose is to quantify the degree to which expectations about GMSST increases may be misleading if based on extrapolation of the linear trend of recent decades.

An 'on-trend' scenario assumes that the post-2010 trend in EEI is the best predictor for the next two decades. This might arise from the absence of effective mitigation of greenhouse gas emissions in combination with continuing reductions in anthropogenic aerosol and/or continuation of recent tendencies in cloud-feedback responses. This is a worst-case scenario.

A 'moderate' scenario has the EEI trend reverting to the pre-2010 slope after 2024. This would be consistent with unmitigated greenhouse gas increases driving a similar evolution of feedback response to that of the 2000s, combined with attributing the recent EEI uptick to reductions in aerosol emissions and/or cloud feedback trends that will not continue hereafter.

The final scenario is 'mitigated'. Here it is assumed that current mitigation policies [44] significantly affect EEI from 2030 onwards. The scenario assumes EEI will stabilise (2030–2035) and thereafter reduce at minus the pre-2010 slope. This progression approximates the time of maximum and the rate of decrease of the central EEI projection from climate models for a strong mitigation scenario (SSP1-2.6) (see supplementary figure 7 in [45]). This SSP1-2.6 scenario is used here to inform a plausible rate of EEI decrease in response to mitigation. However, the EEI is larger than in [45] by ~0.7 W m^{-2} throughout the projected period: the central EEI estimate in SSP1-2.6 is close to 1 W m^{-2} (90% CI: 0.7–1.3) for 2023/4, while the observed EEI was 1.7 W m^{-2} (90% CI: 1.4–2.0) for that period. The mitigated scenario here, informed by observations, therefore lies above the upper 90% confidence interval of EEI for SSP1-2.6.

A caveat to this method of data-driven projection is that the EEA-GMSST coefficient derives from four decades of rising EEI. As EEI stabilises and falls, the value of the coefficient is expected to decrease, as a greater fraction of the EEA accumulates in the deeper oceans. The impact of mitigation on GMSST may therefore be greater than projected here.

The scenarios are shown in figure 3. When integrated in time, these correspond to scenarios for EEA that define three extrapolations of predictor p_3. As noted above, the scenarios are based on EEI trends pre- and post-2010 that themselves are estimated with uncertainty of order 0.1 W m^{-2} decade^{-1}.

Regarding the other predictors: (i) after an illustrative La Niña phase in the initial months of the scenario, neutral ENSO conditions ($p_5 = 0$) are thereafter assumed because there is no long-term predictability, (ii) a zero-mean indicative solar-irradiance cycle with the amplitude of recent cycles is assumed for p_7; and (iii) no major volcanic eruptions are included. The standard deviation of the ENSO index since 1985 (0.88 K) is used to determine an envelope indicating interannual variability around the smoothly evolving GMSSTs of the projections.

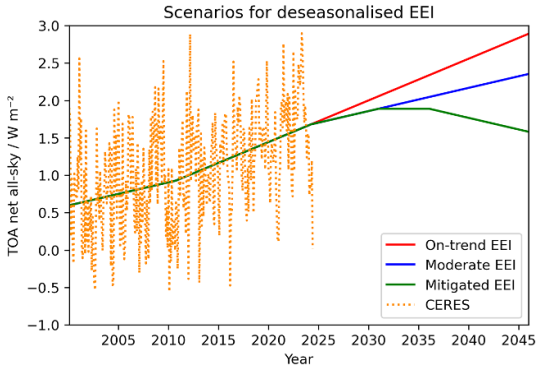

Figure 3. EEI from 2000 to 2024 and three scenarios for the evolution of trends in EEI, used to derive scenarios for future EEA.

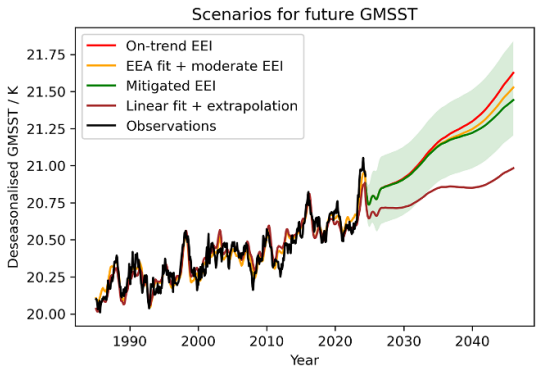

Figure 4. GMSST observations and data-driven future scenarios. The shaded band encompasses 99% of expected ENSO variability around the outer EEI-based scenarios.

The projected GMSSTs are shown in figure 4, accompanied by an extrapolation of the linear GMSST model. Under the 'moderate' scenario and neutral ENSO conditions, the GMSST increase between 2025 and 2045 is 0.78 K (90% CI: 0.63–0.93), which exceeds the 0.53 K neutral-ENSO increase from 1985 to present. Under the 'mitigated' EEI scenario the increase is 0.60 K (90% CI: 0.48–0.72). From extrapolation of the linear fit to the past 40 years one would expect an increase of 0.26 K (90% CI: 0.21–0.31). Thus, even the mitigated scenario projects twice the warming that is implied by linear extrapolation of the trend of recent decades.

These indicative GMSST projections contrast markedly with the results from the untenable linear model for GMSST. These significant differences in data-driven expectations over 21 years illustrate the

need to understand GMSST in relation to EEI and its evolution.

6. Conclusions

Linear extrapolation of the near-GMSST trend of the past four decades is not a reliable basis for expectations of future warming. When interannual variability of GMSST over the past 4 decades is adequately parameterised, an acceleration in the warming trend (a quadratic term) is statistically unambiguous.

Parameterising the GMSST trend as proportional to the EEA is most statistically efficient. This parameterisation has a physical interpretation, that over these decades a near-constant fraction of the EEA has accumulated in the mixed layer, correlating well with SST on decadal timescales. The proportionality between GMSST and EEA is 0.17 ± 0.02 K decade^{-1} W^{-1} m^2. This model explains acceleration in the GMSST as a consequence of the increase in EEI observed over the period.

Using this EEA-based model for GMSST, the record-breaking GMSSTs for 2023 and 2024 can largely be explained by the usual GMSST responses to the El Niño Southern Oscillation and the solar cycle, superimposed on the accelerating trend in response to rising EEI. Without recognising the EEA-driven acceleration, it is difficult to account for ∼0.1 K of the 0.22 K difference in GMSST between the peak months of the 2023/24 El Niño compared to the 2015/16 El Niño.

The EEA-based model for GMSST reflects the EEI circumstances of the past 40 years. The partitioning of energy accumulation within the ocean is dynamic, even on decadal scales, and should be expected to change in future when mitigation policies reverse (hopefully) the upward trend in EEI. Nevertheless, the model can be used to illustrate how GMSST might evolve in the next few decades with reasonable validity.

The key conclusion is that we should not condition our expectations for the rate of surface ocean warming (and therefore of global warming) on linear extrapolation of the GMSST of recent decades. If the EEI trends of recent decades are a guide to the future, the 0.53 K GMSST increase seen over the past 40 years will likely be exceeded in the next 20 years, and by a significant margin in the absence of successful climate mitigation. The warming trend found by this data-driven analysis is faster than model-based estimates applying current policy measures [44], consistent with observed EEI being greater than modelled. It is therefore critical to monitor EEI and to critique the realism of simulated climate projections. Wider society and policy makers should be aware that the rate of global warming over the last four decades is not a guide for the coming decades, otherwise there is a danger of underestimating the urgency of deep reductions in fossil fuel burning.

Data availability statement

No new data were created or analysed in this study.

Acknowledgment

Merchant and Embury were funded by the Natural Environment Research Council [Reference NE/X019071/1, 'UK EO Climate Information Service'], and Allan by the National Centre for Earth Observation, Reference NE/RO16518/1. The authors gratefully acknowledge access to datasets detailed in the Data and Methods section.

ORCID iDs

Christopher J Merchant https://orcid.org/0000-0003-4687-9850
Richard P Allan https://orcid.org/0000-0003-0264-9447
Owen Embury https://orcid.org/0000-0002-1661-7828

References

[1] Cheng L J *et al* 2024 New record ocean temperatures and related climate indicators in 2023 *Adv. Atmos. Sci.* **41** 1068–82
[2] Kuhlbrodt T, Swaminathan R, Ceppi P and Wilder T 2024 A glimpse into the future the 2023 ocean temperature and sea ice extremes in the context of longer-term climate change *Bull. Am. Meteorol. Soc.* **105** E474–E85
[3] Hansen J *et al* 2005 Earth's energy imbalance: confirmation and implications *Science* **308** 1431–5
[4] Allan R P and Merchant C J 2025 Reconciling Earth's growing energy imbalance with ocean warming *Environ. Res. Lett.* **20** 014011
[5] Minobe S, Behrens E, Findell K L, Loeb N G, Meyssignac B and Sutton R 2025 Exceptional climate in 2023–24: beyond the new normal in review
[6] Loeb N G *et al* 2020 New generation of climate models track recent unprecedented changes in Earth's radiation budget observed by CERES *Geophys. Res. Lett.* **47** e2019GL086705
[7] Hodnebrog Ø *et al* 2024 Recent reductions in aerosol emissions have increased Earth's energy imbalance *Commun. Earth Environ.* **5** 166
[8] Goessling H F, Rackow T and Jung T 2025 Recent global temperature surge intensified by record-low planetary albedo *Science* **387** eadq7280
[9] Jenkins S, Smith C, Allen M and Grainger R 2023 Tonga eruption increases chance of temporary surface temperature anomaly above 1.5 °C *Nat. Clim. Change* **13** 127
[10] Schoeberl M R, Wang Y, Ueyama R, Dessler A, Taha G and Yu W 2023 The estimated climate impact of the Hunga Tonga-Hunga Ha'apai eruption plume *Geophys. Res. Lett.* **50** e2023GL104634
[11] Kato S, Rose F G, Rutan D A, Thorsen T J, Loeb N G, Doelling D R, Huang X, Smith W L, Su W and Ham S-H 2018 Surface irradiances of edition 4.0 clouds and the Earth's radiant energy system (CERES) energy balanced and filled (EBAF) data product *J. Clim.* **31** 4501–27
[12] Loeb N G, Doelling D R, Wang H L, Su W Y, Nguyen C, Corbett J G, Liang L, Mitrescu C, Rose F G and Kato S 2018 Clouds and the Earth's radiant energy system (CERES) energy balanced and filled (EBAF) top-of-atmosphere (TOA) edition-4.0 data product *J. Clim.* **31** 895–918
[13] Loeb N G, Lyman J M, Johnson G C, Allan R P, Doelling D R, Wong T, Soden B J and Stephens G L 2012 Observed changes

in top-of-the-atmosphere radiation and upper-ocean heating consistent within uncertainty *Nat. Geosci.* **5** 110–3
[14] Liu C and Allan R P 2018 *Reconstructions of the Radiation Fluxes at the Top of Atmosphere and Net Surface Energy Flux: DEEP-C Version 5.0* (The University of Reading)
[15] Allan R P, Liu C, Loeb N G, Palmer M D, Roberts M, Smith D and Vidale P-L 2014 Changes in global net radiative imbalance 1985–2012 *Geophys. Res. Lett.* **41** 5588–97
[16] C3S Climate indicators sea surface temperature: Copernicus climate change service (available at: https://climate.copernicus.eu/climate-indicators/sea-surface-temperature)
[17] Embury O *et al* 2024 Satellite-based time-series of sea-surface temperature since 1980 for climate applications *Sci. Data* **11** 326
[18] Good S A and Embury O 2024 ESA sea surface temperature climate change initiative (SST_cci): level 4 analysis product, version 3.0 (https://doi.org/10.5285/4a9654136a7148e39b7feb56f8bb02d2)
[19] Johnson G C, Landerer F W, Loeb N G, Lyman J M, Mayer M, Swann A L S and Zhang J 2023 Closure of Earth's global seasonal cycle of energy storage *Surv. Geophys.* **45** 1785–97
[20] Mudelsee M 2019 Trend analysis of climate time series: a review of methods *Earth Sci. Rev.* **190** 310–22
[21] Lean J L and Rind D H 2009 How will Earth's surface temperature change in future decades? *Geophys. Res. Lett.* **36** L15708
[22] van Oldenborgh G J, Hendon H, Stockdale T, L'Heureux M, de Perez E C, Singh R and van Aalst M 2021 Defining El Nino indices in a warming climate *Environ. Res. Lett.* **16** 044003
[23] Montillet J *et al* 2023 Composite PMOD data fusion—updated December 2023, version 1.0 *IEDA* (IEDA)
[24] Nasa/Larc/Sd/Asdc 2018 Global space-based stratospheric aerosol climatology version 2.0
[25] von Schuckmann K *et al* 2023 Heat stored in the Earth system 1960–2020: where does the energy go? *Earth Syst. Sci. Data* **15** 1675–709
[26] Meyssignac B *et al* 2019 Measuring global ocean heat content to estimate the earth energy imbalance *Front. Mar. Sci.* **6** 432
[27] Loeb N G, Ham S-H, Allan R P, Thorsen T J, Meyssignac B, Kato S, Johnson G C and Lyman J M 2024 Observational assessment of changes in Earth's energy imbalance since 2000 *Surv. Geophys.* **45** 1757–83
[28] Baran A J and Foot J S 1994 New application of the operational sounder HIRS in determining a climatology of sulphuric-acid aerosol from the Pinatubo eruption *J. Geophys. Res.* **99** 25673–9
[29] McCormick M P, Thomason L W and Trepte C R 1995 Atmospheric effects of the Mt-Pinatubo eruption *Nature* **373** 399–404
[30] Johnson G C and Lyman J M 2022 GOSML: a global ocean surface mixed layer statistical monthly climatology: means, percentiles, skewness, and kurtosis *J. Geophys. Res.* **127** e2021JC018219
[31] Senapati B, O'Reilly C H and Robson J 2024 Pivotal role of mixed-layer depth in tropical Atlantic multidecadal variability *Geophys. Res. Lett.* **51** e2024GL110057
[32] Hedemann C, Mauritsen T, Jungclaus J and Marotzke J 2017 The subtle origins of surface-warming hiatuses *Nat. Clim. Change* **7** 336
[33] Liang X F, Piecuch C G, Ponte R M, Forget G, Wunsch C and Heimbach P 2017 Change of the global ocean vertical heat transport over 1993–2010 *J. Clim.* **30** 5319–27
[34] Bulgin C E, Merchant C J and Ferreira D 2020 Tendencies, variability and persistence of sea surface temperature anomalies *Sci. Rep.* **10** 7986
[35] Samset B H, Lund M T, Fuglestvedt J S and Wilcox L J 2024 2023 temperatures reflect steady global warming and internal sea surface temperature variability *Commun. Earth Environ.* **5** 460
[36] Minière A, von Schuckmann K, Sallee J-B and Vogt L 2023 Robust acceleration of Earth system heating observed over the past six decades *Sci. Rep.* **13** 22975
[37] Schwartz S E 2007 Heat capacity, time constant, and sensitivity of Earth's climate system *J. Geophys. Res.* **112** D24S05
[38] Bellouin N *et al* 2020 Radiative forcing of climate change from the Copernicus reanalysis of atmospheric composition *Earth Syst. Sci. Data* **12** 1649–77
[39] Yuan T L *et al* 2024 Abrupt reduction in shipping emission as an inadvertent geoengineering termination shock produces substantial radiative warming *Commun. Earth Environ.* **5** 281
[40] Quaas J *et al* 2022 Robust evidence for reversal of the trend in aerosol effective climate forcing *Atmos. Chem. Phys.* **22** 12221–39
[41] Kramer R J, He H Z, Soden B J, Oreopoulos L, Myhre G, Forster P M and Smith C J 2021 Observational evidence of increasing global radiative forcing *Geophys. Res. Lett.* **48** e2020GL091585
[42] Jenkins S, Povey A, Gettelman A, Grainger R, Stier P and Allen M 2022 Is anthropogenic global warming accelerating? *J. Clim.* **35** 4273–90
[43] Gettelman A, Christensen M W, Diamond M S, Gryspeerdt E, Manshausen P, Stier P, Watson-Parris D, Yang M, Yoshioka M and Yuan T 2024 Has reducing ship emissions brought forward global warming? *Geophys. Res. Lett.* **51** e2024GL109077
[44] Duan L and Caldeira K 2024 Rate of global warming projected to decline under current policy *Environ. Res. Lett.* **19** 092001
[45] Meyssignac B *et al* 2023 How accurate is accurate enough for measuring sea-level rise and variability *Nat. Clim. Change* **13** 796